

Modulation of Cerebellar Cortical Plasticity Using Low-Intensity Focused Ultrasound for Poststroke Sensorimotor Function Recovery

Neurorehabilitation and Neural Repair

1–11

© The Author(s) 2018

Reprints and permissions:

sagepub.com/journalsPermissions.nav

DOI: 10.1177/1545968318790022

journals.sagepub.com/home/nnr



Hongchae Baek, MSc^{1,2}, Ki Joo Pahk, PhD¹, Min-Ju Kim¹,
Inchan Youn, PhD^{1,2}, and Hyungmin Kim, PhD^{1,2} 

Abstract

Background. Stroke affects widespread brain regions through interhemispheric connections by influencing bilateral motor activity. Several noninvasive brain stimulation techniques have proved their capacity to compensate the functional loss by manipulating the neural activity of alternative pathways. Over the past few decades, brain stimulation therapies have been tailored within the theoretical framework of modulation of cortical excitability to enhance adaptive plasticity after stroke. **Objective.** However, considering the vast difference between animal and human cerebral cortical structures, it is important to approach specific neuronal target starting from the higher order brain structure for human translation. The present study focuses on stimulating the lateral cerebellar nucleus (LCN), which sends major cerebellar output to extensive cortical regions. **Methods.** In this study, in vivo stroke mouse LCN was exposed to low-intensity focused ultrasound (LIFU). After the LIFU exposure, animals underwent 4 weeks of rehabilitative training. **Results.** During the cerebellar LIFU session, motor-evoked potentials (MEPs) were generated in both forelimbs accompanying excitatory sonication parameter. LCN stimulation group on day 1 after stroke significantly enhanced sensorimotor recovery compared with the group without stimulation. The recovery has maintained for a 4-week period in 2 behavior tests. Furthermore, we observed a significantly decreased level of brain edema and tissue swelling in the affected hemisphere 3 days after the stroke. **Conclusions.** This study provides the first evidence showing that LIFU-induced cerebellar modulation could be an important strategy for poststroke recovery. A longer follow-up study is, however, necessary in order to fully confirm the effects of LIFU on poststroke recovery.

Keywords

low-intensity focused ultrasound, photothrombosis, recovery, rehabilitation, cerebellum, stroke

Introduction

Stroke remains one of the most common causes of long-term sensorimotor impairment and ranks as the second leading cause of death worldwide.¹ There are 2 major types of stroke, ischemic and hemorrhagic. Ischemic stroke is due to the obstruction of blood flow to the brain, whereas hemorrhagic stroke occurs when a blood vessel ruptures. Most strokes are ischemic in nature and hemorrhagic stroke is responsible for only 15% of all stroke deaths.² In modern medicine, given the time-sensitive nature of acute stroke therapy, current treatment strategies for stroke focus on reducing the size of ischemic damage and rapid recanalization of the ischemic stroke lesion. Among many, intravenous thrombolysis using recombinant tissue plasminogen activator, known as rt-PA, is the only Food and Drug

Administration–approved acute ischemic stroke medication,³ and is currently the most effective therapy for patients.⁴

¹Center for Bionics, Biomedical Research Institute, Korea Institute of Science and Technology, Seoul, Republic of Korea

²Division of Bio-Medical Science & Technology, KIST School, Korea University of Science and Technology, Seoul, Republic of Korea

Supplementary material for this article is available on the *Neurorehabilitation & Neural Repair* website at <http://nnr.sagepub.com/content/by/supplemental-data>.

Corresponding Author:

Hyungmin Kim, Center for Bionics, Biomedical Research Institute, Korea Institute of Science and Technology, 5, Hwarang-ro 14-gil, Seongbuk-gu, Seoul 02792, Republic of Korea.

Email: hk@kist.re.kr

Yet, due to the narrow 3-hour therapeutic time window, the accessibility of rt-PA is restricted to only 5-10 % of the population.⁵ Also, a correlation between antiplatelet therapy in combination with rt-PA thrombolysis in ischemic stroke (ARTIS) and intracranial hemorrhage has been strongly suggested.^{6,7} In addition to this, there is a concern that development of new pharmacotherapeutics is providing diminishing returns in clinical medicine,⁸ prompting research into developing nonpharmacological therapies such as non-invasive brain stimulation.

Brain stimulation techniques can exert neuromodulatory effect on surviving tissue as a means of boosting cortical reorganization in the ischemic brain. Noninvasive neurostimulators such as transcranial magnetic stimulation (TMS) and transcranial direct current stimulation (tDCS) are capable of promoting functional recovery in treating neurological conditions including stroke.⁹ None of these techniques, however, can stimulate deep subcortical structures without influencing surrounding or intervening neural tissue. More recently, low-intensity focused ultrasound (LIFU)-mediated neuromodulation has been introduced as an alternative because of its bimodal capability (ie, excitation and inhibition) and superior spatial resolution and penetrability.¹⁰ In 2008, a pioneering work was published by Tyler's group¹¹ showing that ultrasound (US) is capable of activating synaptic transmission by directly evoking intracellular calcium and sodium ion influx. Subsequently, a growing body of literatures have shown successful elicitation of motor behavior in response to US-induced sensorimotor cortical stimulation in mice¹²⁻¹⁵ and rats.^{15,16} Several potential neuroprotective mechanisms of LIFU have been demonstrated to promote cerebral blood flow after the ischemic injury.¹⁸ Furthermore, it has been reported that LIFU-mediated preconditioned endothelial cells could lead to the reduction of the synthesis of thrombus with increased ischemic tolerance by downregulating metabolism.¹⁹

Poststroke recovery is essentially associated with the process of functional and structural changes of the brain known as brain plasticity, which takes place at multiple levels from cellular to cortical reorganization. One of the most popular approaches to maximize motor recovery involves stimulating primary motor cortex (M1) in the ipsilesional hemisphere and/or suppressing the excitability of the contralesional hemisphere to restore the balance between competing hemispheres. However, contrary to the classical interhemispheric inhibition model, plasticity of ipsilateral M1 turned out to diverge based on the degree and the nature of the ischemic injury.²⁰ In fact, large-scale studies on patients with diverse location, lesion size, and variability of injury to ipsilateral M1 have reported worse rehabilitation outcomes with current stimulation therapy.²¹ Thus, it was not surprising when patients with greater brain damage failed to induce motor evoked responses from stimulating ipsilateral M1.²² Our study was initially developed from

previous studies reporting the efficacy of electrical^{23,24} or optical²⁵ stimulation of the lateral cerebellar nucleus (LCN) in the treatment of stroke. Our hypothesis is that ultrasound stimulation of the LCN, rather than electrical or optical stimulation, would improve rehabilitation metrics after stroke, in vivo and benefit from its noninvasiveness and clinical utility. Afferent output from the LCN, the largest and most lateral from the midline of the 4 pairs of the deep cerebellar nuclei, is connected to impaired cerebral cortex via dentothalamocortical (DTC) pathway. This pathway begins in the cerebellar cortex of the lateral zone of the cerebellum, and passes to the dentate nucleus, then to the thalamus, and finally to the cerebral cortex. Stimulation of LCN allows effective activation of the peri-infarct zone, delivering therapeutic impact over a much larger perilesional circuitry via a natural afferent pathway from the cerebellum.²⁶ In addition, acute brain injury accompanied by cerebral infarction generally reduces blood flow and metabolism in the contralateral cerebellum. This phenomenon, named crossed cerebellar diaschisis (CCD), is an immediate reaction to cerebellum deactivation due to reduced input from the contralateral cerebral cortex. Hence, it is plausible to pursue a strategy of compensating disrupted efferent and excitatory output from crossed cerebral cortex in order to restore decreased neuronal activity in functionally connected cerebellum.²⁷

In this study, we aim to investigate 4-week follow-up results of LIFU-induced stimulation of LCN in an acute photothrombotic animal stroke model. Motor-evoked potential (MEP) responses and motor movement in forelimb were measured by LIFU cerebellar neuromodulation of contralateral motor cortex through the DTC pathway. The balance beam test was used to evaluate balance control and locomotor performance and sensorimotor asymmetry was examined with the adhesive removal test. Therapeutic effects of LIFU on alleviating brain edema were also investigated. Finally, potential tissue damage due to LIFU stimulation was carefully assessed histologically using hematoxylin and eosin staining.

Methods

Animal Preparation

Male ICR mice (4-5 weeks old, 28-32 g) were used in our experiments. The animals were housed in a temperature-controlled room (22°C ± 2°C) with constant humidity of 45% to 50%, alternate light/dark conditions (a 12-hour light/dark cycle, light on 07:00-19:00 hours) and food and water ad libitum. All surgical procedures were carefully reviewed and approved by the institutional board permission obtained from the Animal Care and Use Committees at Korea Institute of Science and Technology. Mice were randomly assigned to 3 groups: control, stroke, and stroke + LIFU. The animals in the stroke + LIFU group were subjected to 2 successive

Table 1. Modified Neurological Severity Score Grading System.

Normal	Grade 0:	No observable deficit
Moderate	Grade 1:	Occasional foot faults on the beam walking
Severe	Grade 2:	Circling toward the side of lesion
	Grade 3:	Depressed level of consciousness with circling
	Grade 4:	Unresponsive to stimulation or death

20-minute long LIFU stimulations separated by 20-minute rest intervals 1 day after the stroke, whereas LIFU stimulation was not applied to the stroke group. The majority of previous stroke rehabilitation applied a 20-minute session of tDCS.²⁸⁻³⁰ We therefore conducted 20-minute sessions with a 20-minute resting interval in order to maximize the LIFU treatment effect. Finally, animals in the control group underwent sham surgical procedure, which included general anesthesia and scalp incision only. All experiments were performed under ketamine-xylazine general anesthesia.

Photothrombosis Procedure

The animals used in our experiments were anesthetized with 80 mg/kg ketamine and 10 mg/kg xylazine mixture by intraperitoneal injection. To induce photothrombosis, a light-sensitive dye, Rose Bengal (Sigma, Milan, Italy), was prepared at a concentration of 10 mg/mL right before the surgery and then a dose of 10 μ L/g of body weight was injected intraperitoneally. After a 5-minute interval for the dye to diffuse into the bloodstream, cold white light was illuminated on the desired skull surface (anterior-posterior [AP] -0.02 and medial-lateral [ML] -2.00 mm from bregma) for 7.5 minutes using a fiber-optic light source (Photonic PL3000, Photonic Optics, UK) with an unfiltered 150 W halogen bulb (Philips, 13629, 21V150W, Japan). After receiving the photothrombotic surgery, all animals were evaluated with the neurological severity score (NSS) test to examine the behavior deficits and screened for NSS score grade 2. We performed NSS test slightly modified from that used in Bederson et al,³¹ whereby a 0-4 grading scale was used to control the severity of ischemic injury among the groups (Table 1).

Sonication of LCN

A schematic diagram of the in vivo LIFU experimental setup used in this study is shown in Figure 1B. A 0.35 MHz single element bowl-shaped focused US transducer (GPS350-D25_FL25, The Ultrason Group, USA) with an aperture size of 25 mm, a focal length of 23.85 mm and lateral and axial full width at half maximum (FWHM) dimensions of 5.5 mm and 29.8 mm (Figure 1F), was employed in our experiments.

The focal length and the FWHM dimensions were experimentally measured in degassed and deionized water under linear propagation conditions with a calibrated hydrophone (ONDA Corp, HNR-0500, CA, USA) at a spatial step size of 0.5 mm. The transducer was driven by 2 function generators (33210A, Agilent, Santa Clara, CA) via a linear radio frequency power amplifier (240L, ENI Inc, Rochester, NY, USA). The LIFU exposure conditions used in our experiments were as follows: 50 % duty cycle, 1-kHz pulse repetitive frequency (PRF), 0.5 ms tone burst duration (TBD), 300-ms sonication duration (SD), 2-second interstimulus interval (ISI), and a spatial-peak pulse-average intensity (I_{sppa}) of 2.54 W/cm² (Figure 1C). The acoustic intensity used in our study was reported as the key parameter for effectively eliciting electromyographic response in mouse with 50% success rate.¹³ This sonication parameter was verified for eliciting movements with in vivo experiments reported earlier.¹⁶

The LCN was the target brain region during the experiments. The transducer holder attached to a moving arm (LX Desk Monitor Arm, ERGOTRON, USA) was placed directly on the exposed skull and the acoustic field coupled through a 100- μ m thick acoustically transparent polyethylene (Mylar) film. The holder was designed such that the distance from the tip of the holder to the center of the transducer surface was 20 mm. The LIFU focus was, therefore, 3.85 mm below the surface of the exposed skull. As shown in Figure 1E, we positioned the transducer according to the target coordinates from bregma (ie, AP -6.00 mm, ML -2.2 mm, and dorsal-ventral [DV] -3.75 mm).³²

Electromyography

For electromyogram (EMG) measurement, 2 subdermal wire electrodes (SWE-L25, Ives EEG Solution, MA, USA) were inserted into both sides of forelimb triceps brachii muscles. Also, an extra electrode was placed on the tail which served as a reference. Each wire lead was connected to a data acquisition system (PL3508, Model ML138, ADInstruments, Sydney, Australia). The EMG signal was recorded at a 2 kHz sampling rate (band-pass filter, 10 Hz to 1 kHz) using LabChart Software (ADInstruments, Sydney, Australia) with the 60 Hz notch filter active. MEPs were generated serially, consisting of 30 trials per 1-minute block, at 2-second intervals in the forelimb musculature time-locked to the onset of the cerebellar LIFU stimulation.

MEP Data Processing and Analysis

Repetitive sonication of LCN over the first 20-minute LIFU session generated 600 consecutive MEP responses in sync with the cerebellar stimulation every 2 seconds. Each of 5 consecutive MEP responses (ie, approximately 10 seconds)

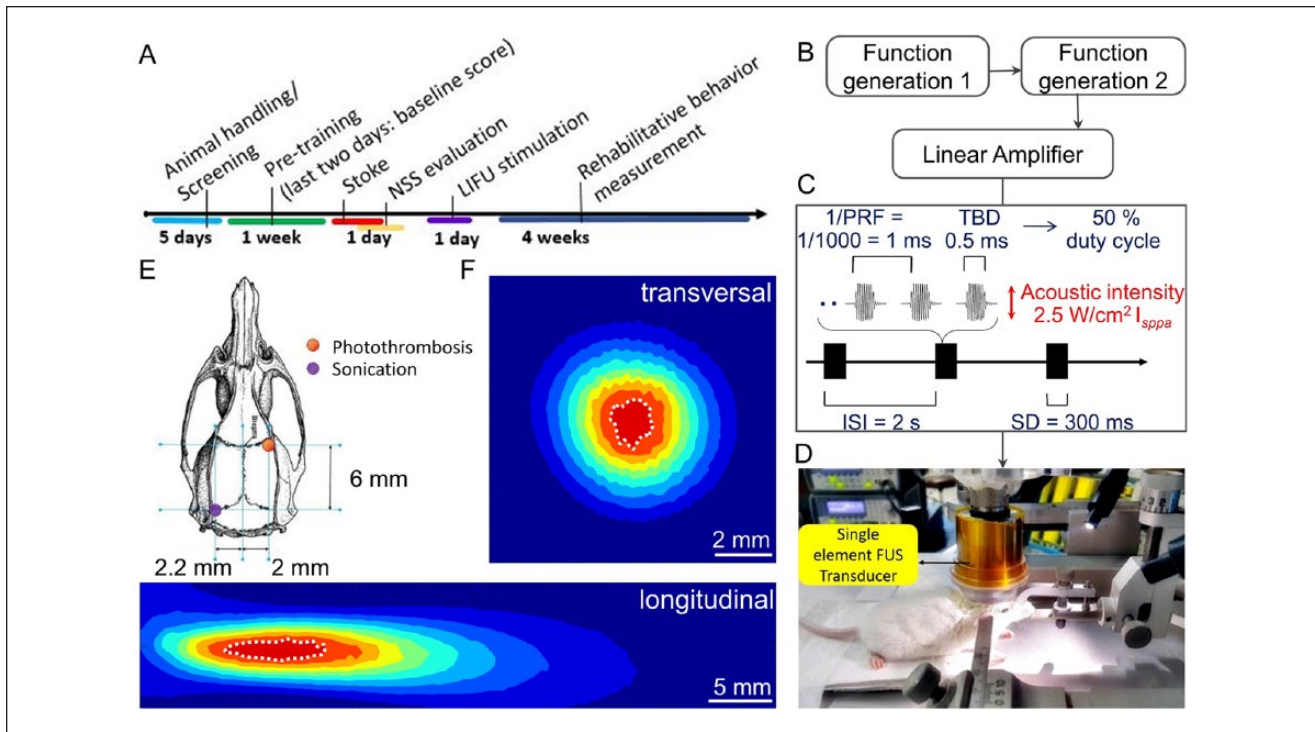


Figure 1. Experimental diagram used in our study. (A) Six weeks of the experimental procedure are described. (B) A schematic diagram of the low-intensity focused ultrasound (LIFU) stimulation system used is shown. (C) Sonication parameter used in the study is illustrated with definitions: pulse-repetition frequency (PRF), tone-burst duration (TBD), duty cycle (DC), sonication duration (SD), interstimulus interval (ISI), and spatial-peak pulse-average intensity (I_{sppa}). (D) Experimental setup used to stimulate the lateral cerebellar nucleus (LCN) in mouse is shown. (E) The location of sonication and the photothrombotic stroke (F) experimentally measured acoustic intensity profiles along the transversal (upper) longitudinal (lower) directions. The full-width of 90%-maximum of the acoustic intensity field is circled with the white dotted lines.

was grouped together as the running average of an MEP window. Root mean square (RMS) ratio of each window was calculated and then normalized to the baseline data of initial “OFF” stimulation period by dividing each data point by the mean of the “OFF” segment value. Following an initial prestimulation “OFF” period, MEPs in right forelimb were elicited during the first 20-minute LCN stimulation. An intervening “OFF” period after the first session, served as a washout period for checking the reversible effect of LIFU on LCN stimulation. In the second session, MEPs from the left forelimb were recorded in response to the cerebellar LCN stimulation.

Balance Beam Test

In this study, animals’ motor coordination and balance were assessed using a custom-made 125 cm long and 1 cm wide beam. Ledges (1 cm wide) were placed on both sides along the beam to (Figure 2B) provide a crutch for contralesional weight bearing steps as well as to avoid reliance on nonimpaired limbs to compensate the impairment.³³ Additionally, walking speed was measured over a distance of about 125

cm on the last day of the pretraining session, which was used as a baseline score. The evaluation of poststroke behavior started the day after the stroke surgery for the stroke group ($n = 12$) and it commenced after the sonication for the stroke + LIFU group ($n = 12$). Balance beam test in control group ($n = 9$) was also conducted for comparison.

Adhesive Removal Test

An adhesive removal test is a common method to evaluate sensorimotor asymmetries resulting from stroke-related unilateral brain damage.³⁴ During our experiments, 2 identical pieces of adhesive tape (3 mm × 4 mm) were gently applied on the forepaws (Figure 3C). Sensorimotor performance was investigated by measuring the time required to remove the adhesive from each paw (ie, time-to-remove). To evaluate the recovering functional symmetry between both forelimbs, asymmetry scores were calculated as follows: $((\text{contralateral time-to-remove}) - (\text{ipsilateral time-to-remove})) / ((\text{contralateral time-to-remove}) + (\text{ipsilateral time-to-remove}))$. Animals with unilateral brain damage show a bias for faster time-to-remove from the unimpaired

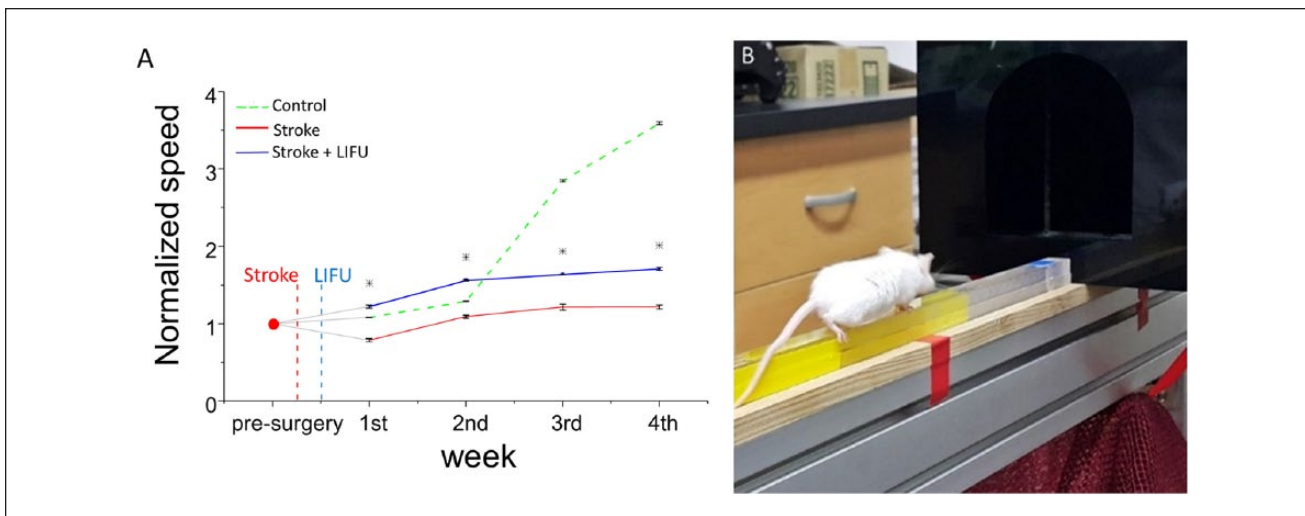


Figure 2. (A) Experimentally measured walking speed using the balance beam test. Control group shows a sharp increase from the second week. In our study, at least 2 weeks was needed for mice to start learning the complex coordinated movement on the balance beam. (B) An example showing a mouse crossing the beam toward a dark box.

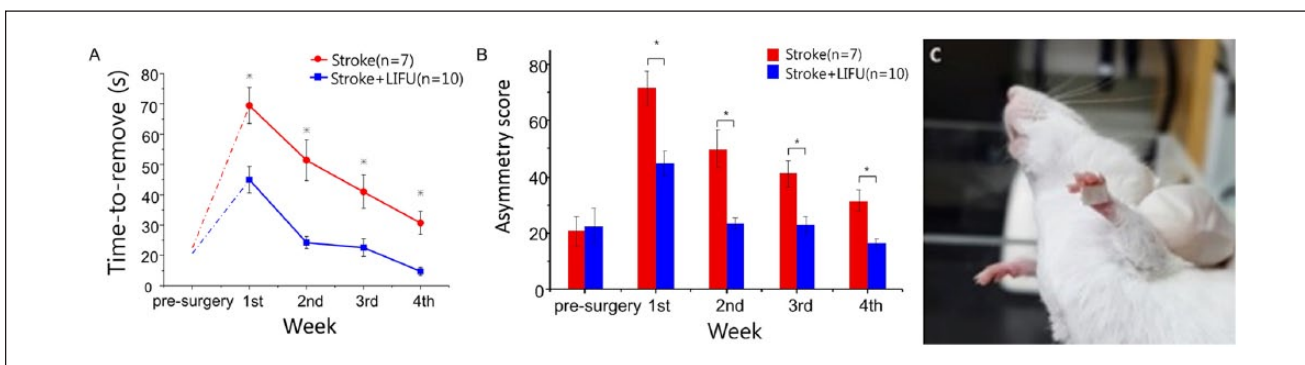


Figure 3. Adhesive removal test used in this study. (A) shows the improvement of the time-to-remove score obtained only from the affected side (contralateral forelimb). The time-to-remove score in the contralateral limb is significantly reduced in the stroke + low-intensity focused ultrasound (stroke + LIFU) group after the stroke followed by the LIFU insonation. On the other hand, (B) shows the relieved imbalance between the affected and the unaffected sides regarding the tape removal speed. The graph compares the asymmetry in 2 groups. In the stroke + LIFU group, the asymmetry score was returned to its presurgery baseline score in 2 weeks, whereas the stroke group maintained the score above the presurgery level until the end of the fourth week. (C) An example of adhesive tape on mouse's forepaw is shown.

ipsilateral forelimb. Animals (stroke group, $n = 7$; stroke + LIFU group, $n = 10$) were trained for 4 days before the surgery and only 1 trial was conducted per day according to the protocol described in Bouet et al.³⁵ We performed a blind test by randomly selecting animals either from the stroke + LIFU or the stroke group.

Evaluation of Brain Edema

The degree of cerebral edema was examined and compared between the stroke ($n = 7$) and the stroke + LIFU ($n = 5$) groups by calculating the percentage change of increased brain water content and tissue swelling. The brains were

extracted three days after the photothrombotic stroke in the stroke group. For the stroke + LIFU group, the brains were extracted 2 days after the LIFU session (also 3 days after the photothrombotic stroke). The extracted brains were dissected into the ipsilateral hemisphere (IH) and contralateral hemisphere (CH) to the infarcts. Wet weight and dry weight of hemispheres were measured before and after they were dehydrated in an oven for 3 days at 75°C. First, both IH and CH brain water content expressed as percentage water content = $100 \times (\text{wet weight} - \text{dry weight}) / \text{dry weight}$ were calculated for assessing percentage change of increased water content in IH. In addition, according to the equation described in Keep et al.,³⁶ initial wet weight was calculated

using the contralateral water content and final ipsilateral dry weight. Initial wet weight of the ipsilateral sample = (contralateral cortical water content + 1) * final ipsilateral dry weight. Consequently, the impact of brain edema on tissue swelling was calculated as percentage tissue swelling = $100 * (\text{final wet weight} - \text{initial wet weight}) / \text{initial wet weight}$.

Histological Assessment

The LCN of 3 healthy mice were exposed to LIFU with the same exposure parameters used for the stroke + LIFU group. The animals were euthanized on the next day for histological observation. After sacrifice, they were perfused intracardially with buffered 4% paraformaldehyde followed by postfixation in that solution at 4°C overnight. The brains were cryoprotected and 30- μm sagittal sections were obtained in a cryostat. Cerebellar structure was examined for neuronal loss or cell structure changes resulting from the LIFU exposure. Histological examination was performed by staining the sections with hematoxylin and eosin.

Statistics

All analyses were performed using the SPSS Statistics (version 20, IBM Corp, Armonk, NY, USA). All the behavior data collected from the beam balance and the adhesive removal tests were statistically analyzed by either 2-way repeated-measures analysis of variance (ANOVA) with “treatment group” (the control, stroke + LIFU, and the stroke groups) and “period” (first, second, third, and fourth week of the LIFU experiment) as within-subjects factors followed by Scheffe’s post hoc test. Greenhouse-Geisser corrected values were used when data violated the assumption of sphericity. Finally, the brain edema data were statistically analyzed by 1-way ANOVA. In our study, a P value less than .05 was considered statistically significant.

Results

Balance Beam Test

The experimentally measured walking speed plotted in Figure 2A clearly showed that there are significant differences among the 3 groups, that is, $F(2, 16) = 46.640, P < .005$; control = $2.214 \pm 0.185, n = 9$; stroke + LIFU = $1.436 \pm 0.366, n = 12$; stroke = $0.969 \pm 0.260, n = 12$. Post hoc analysis revealed that the average walking speed of the animals in the stroke + LIFU group was significantly faster than that of the stroke group, that is, $F(1, 11) = 7.659, P < .05$. In addition, a significant interaction between the treatment groups and time periods was observed with $F(6, 48) = 66.710, P < .005$. Post hoc test revealed that the walking speed in the stroke + LIFU group stayed significantly higher

than those in the stroke group during the entire 4 weeks of the experimental period (Figure 2A), that is, first week, $F = 8.648, P < .05$; second week, $F = 6.614, P < .05$; third week, $F = 5.632, P < .05$; and fourth week, $F = 8.039, P < .05$.

Adhesive Removal Test

Figure 3 shows that the stroke + LIFU group took much shorter time to remove the adhesives than the stroke group over the 4 weeks, that is, $F(1, 6) = 10.141, P < .05$; stroke + LIFU = $26.06 \pm 11.821, n = 10$; stroke = $48.901 \pm 20.972, n = 7$. No significant interaction was found between the “treatment group” and the “period,” $F(3, 18) = 0.842$, non-significant. At each week, the stroke + LIFU group showed significantly faster time-to-remove scores compared with those in the stroke group, that is, first week, $F = 6.532, P < .05$; second week, $F = 5.100, P < .05$; third week, $F = 5.667, P < .05$; and fourth week, $F = 7.213, P < .05$. Furthermore, the asymmetry score comparison yielded a significant difference between the stroke + LIFU and the stroke groups, $F(1, 6) = 11.157, P < .05$; stroke + LIFU = 25.397 ± 9.775 ; stroke = 48.424 ± 14.337 . A 2-way repeated-measures ANOVA revealed no interaction, $F(3, 18) = 1.010$, non-significant, between the “treatment group” and the “period.” We observed significantly reduced asymmetry score in the stroke + LIFU at each week, that is, first week, $F = 17.558, P < .05$; second week, $F = 6.337, P < .05$; third week, $F = 5.518, P < .05$; and fourth week, $F = 7.515, P < .05$.

Brain Edema

Photothrombotic stroke in mice resulted in increased water content in IH. The increased water percentage change in IH compared with those in CH was considered as an indicator of cerebral hemisphere asymmetry with regard to edema, as shown in Figure 4A. The LIFU treatment in cerebellar LCN significantly lowered the percentage change in increased water content and tissue swelling in IH. That is, % change, $F = 6.780, P < .05$; stroke = $29.741 \pm 30.187, n = 7$ versus stroke + LIFU = $22.668 \pm 8.515, n = 5$; tissue swelling, $F = 6.021, P < .05$; stroke = 23.517 ± 18.898 versus stroke + LIFU = 18.218 ± 5.658 .

Histological Assessment

Histological observation of the tissue samples obtained from the whole cerebellum revealed no sign of bleeding or tissue damage (Figure 4B).

Discussion

In this study, we examined the effect of LIFU stimulation on the mouse in vivo DTC pathway by targeting its origin in the LCN as a neurorehabilitative therapy. The experimental

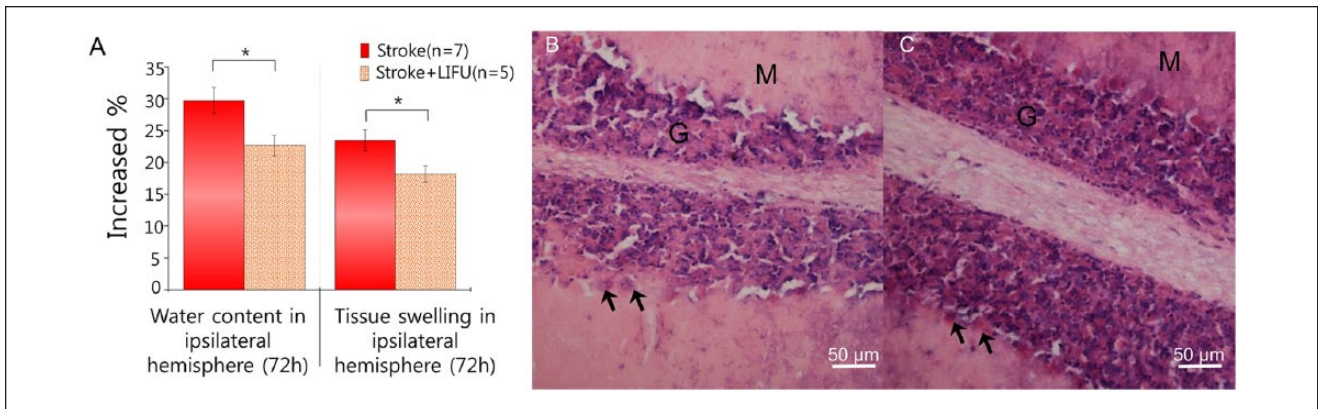


Figure 4. (A) Increased percentage of water content and tissue swelling in ipsilateral hemisphere. The increased % of water content as well as tissue swelling in ipsilateral hemisphere were significantly higher in the stroke group compared with those in the stroke + low-intensity focused ultrasound (stroke + LIFU) group. (B) Hematoxylin and eosin-stained sections of mouse cerebellar structure showing molecular layer M and granular layer G. Hematoxylin and eosin-stained normal mouse cerebellum showed normal Purkinje cells. (C) No sign of damage or bleeding found in the whole cerebellum. Photomicrograph of hematoxylin and eosin-stained histological sections (C) of mice exposed to LIFU revealed normal linear distribution of Purkinje cell layer (indicated by the black arrows).

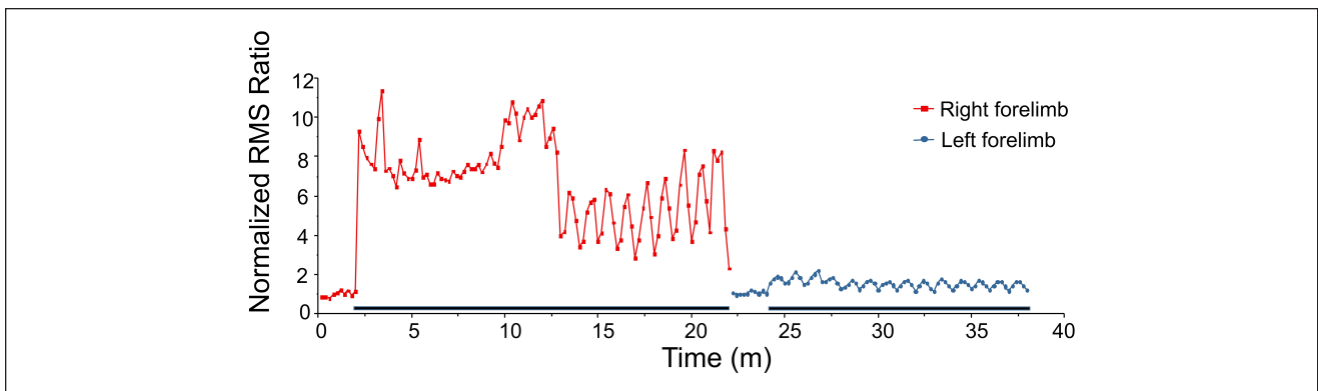


Figure 5. Motor-evoked potential (MEP) induction during the low-intensity focused ultrasound (LIFU) sessions. The difference of the MEP amplitude between the affected (blue) and the unaffected forelimbs (red) induced by the cerebellar LIFU stimulation might be due to the possible damage of neural circuits by the photothrombotic stroke. The dark bars on the time scale indicate the sonication “ON” time.

results presented in this study convincingly showed that the mice exposed to LIFU after the photothrombotic stroke exhibited enhanced sensorimotor performance compared to the stroke group. These results support our hypothesis that LIFU could enhance plasticity in spared cortical tissue by stimulating the contralesional LCN, thereby facilitating the functional reorganization of the perilesional cortical areas.

The underlying mechanism for motor recovery following stroke is closely linked with the perilesional functional reorganization across species.³⁷⁻⁴⁰ Patients undergoing post-stroke rehabilitative treatment have demonstrated improved motor performance of the paretic limb associated with significantly enlarged cortical representation of the muscle output in the affected hemisphere determined by TMS.⁴⁰⁻⁴²

These studies showed that TMS is capable of instigating neural reorganization by altering cortical excitability in the secondary motor cortex of the affected hemisphere as measured by MEP generation along with motor movement. Several studies reported that LCN electrical stimulation can elicit cortical excitability in a frequency-dependent manner and produced the strongest MEP with 30-Hz stimulation.^{23,43} Our MEP results shown in Figure 5 indicate the involvement of lateral cerebellum together with cerebral motor cortex in the process of the LIFU therapeutic effect in recovering from ischemic injury. The repeated variability of the MEP amplitude at approximate 1-minute time scale is thought to be due to the results from decreased muscle reaction to compensate for the fatigue in response to the ultrasound

induced stimulation. This repeated time scale is consistent with previously reported evoked EMG-torque relationship due to fatigue.⁴⁴ In our study, we observed forelimb movements from both sides during the LIFU LCN stimulation (Supplementary Video 1, available in the online version of the article).

Here, we demonstrate that early treatment of LIFU neurostimulation of LCN can yield compensatory activation in balance, coordination, and sensorimotor skills, and more importantly, persistently sustain improvement 4 weeks after the stimulation (Figures 2 and 3). The results of electrical stimulation of LCN for poststroke recovery^{23,24} also showed similar functional outcome to our study. Cooperrider et al²⁴ showed that rats with LCN electrical stimulation at 2 weeks poststroke were as capable as they were at prestroke performance in pasta retrieval performance. Similarly, mice with optogenetically stimulated LCN after stroke also exhibited significantly enhanced performance in a beam rotating test with scores nearly recovered to the baseline prestroke state at 2 weeks poststroke.²⁵ Despite the difference in stroke models and behavioral measurements, these recovery time points coincide with our data. LIFU stimulated mice exhibited a prestroke level of asymmetry in adhesive removal test at 2 weeks poststroke (Figure 3B), and the slope of recovery rate was at the highest in terms of time-to-remove score also 2 weeks after the stroke (Figure 3A). In addition, the walking speed in the LIFU + stroke group was even faster than that of the control group in beam walking test until 2 weeks after the stroke (Figure 2A). The potential mechanisms of the improved level of functioning after the neural damage is the compensatory augmentation, which is supported by the theory of paradoxical functional facilitation.⁴⁵

The prognosis of poststroke recovery is most highly correlated with the resolution of brain edema and fast restoration of the blood flow of penumbra tissue through encouraging the neighboring circulation.⁴⁶ Whereas neuronal death begins instantly after the stroke at the ischemic core, tissue damage and edema progress for few days in the penumbra, giving few days of crucial therapeutic window for intervention. The reduction of brain edema is largely counting on the vasodilation, which can facilitate the absorption of interstitial excessive fluids from the injured cells in penumbra. Numerous *in vivo* and *in vitro* studies regarding the US-mediated vasodilation using various frequency ranges (0.02-3.0 MHz) have been reported.⁴⁷ They hypothesized that ultrasound can increase endothelial nitric oxide synthesis (eNOS) and neuronal nitric oxide synthesis (nNOS) activity via US-induced shear stress on the vessel wall, resulting in the enhancement of the cerebral blood flow by dilating vessels and collaterals. Our results of reduced brain edema and tissue swelling in the affected hemisphere (Figure 4A) show that LIFU stimulation of LCN was neuroprotective in the interconnected cerebral

motor cortex. These results address that LCN can be a potential LIFU stimulation target for producing abscopal effect on anatomically distant widespread peri-infarct regions through the DTC pathway. In humans, noninvasive cerebellar stimulation exerted heterosynaptic M1 plasticity, allowing therapeutic manipulation of impaired cortical plasticity in the future.⁴⁸ Proville et al⁴⁹ examined the impact of cerebellar input in cortical regions. Optogenetic stimulation of cerebellar Purkinje cells exhibited inhibited cerebellar nuclei, followed by excitation in neurons in thalamus and motor cortex through the ascending cerebello-thalamo-cortical pathway.⁴⁹ A previous study²⁵ has shown that an increased expression of GAP43, a plasticity marker, in ipsilesional somatosensory and motor cortex, the LCN stimulation can produce a positive outcome in promoting plasticity in contralateral cortical area, which correlates with functional recovery. Recently, a critical finding of a structural link between the cortical motor area and the cerebellum provided an important role for cortical-cerebellar pathway in poststroke rehabilitation.⁵⁰ Future investigations will be focused on elucidating the importance of cortical remapping linked with cortical-cerebellar circuit dynamics in stimulation-induced poststroke recovery.

The largest confounding factor in this study is most probably the ancillary excitatory input on other cerebellar cortex cells throughout the three distinct layers due to the larger LIFU focal size than the size of the targeted deep cerebellar nuclei (ie, LCN). However, it has been reported that actual FUS-mediated neuromodulatory area is more localized, close to be full-width at 90%-maximum of the acoustic intensity field.⁵¹ Precise neural-specific stimulation could be achievable by using a multi-element transducer system. In addition, superior target precision of LIFU-mediated neuromodulation can be achieved using much higher frequency (ie, 1.9 MHz)⁵² or by modifying relatively high-frequency carrier signal with low-frequency ultrasound.¹⁵ Excitatory afferent neurons synapse with granule cells in granule cell layer. Parallel fibers of granule cells synapse with molecular layer interneurons, including both stellate and basket cells. Both interneurons and cerebellar Golgi cells serve strong inhibition onto the Purkinje cells and so do the Purkinje cells to the deep cerebellar nuclei, LCN.⁵³ These inhibitory forces onto the Purkinje cell layer are thought to balance the cerebellar cortical output if the excitation becomes too wide.

Finally, we elicited forelimb movement with the intensity I_{sppa} of 2.5 W/cm² (ie, spatial-peak temporal-average intensity I_{spta} of 1.25 W/cm²) and mechanical index (MI) of 0.54. Acoustic intensities used in our study comply with the upper limit specified by the Food and Drug Administration for diagnostic imaging devices ($I_{sppa} < 190$ W/cm², MI < 1.9) and the International Electrotechnical Commission (IEC) for US physiotherapy device.⁵⁴ To calculate temperature rise due to the sonication, we adopted the equation used

in a previous study⁵⁵ ($\Delta T = 2\alpha It/\rho_b C_p = 2 \times 0.05 \text{ cm}^{-1} \times 1.25 \text{ W cm}^{-2} \times 0.3 \text{ s}/3.796 \text{ J cm}^{-3} \text{ }^\circ\text{C}^{-1} = 0.009^\circ\text{C}$, where α = the absorption coefficient, I_{spta} = the acoustic intensity in focal region, t = the pulse duration, ρ_b = the density of brain tissue and C_p = the specific heat of brain tissue) and confirmed that the LIFU-induced temperature rise is below the value of 43°C , which causes thermal bioeffects of US.⁵⁶ However, Younan et al¹⁶ numerically showed that reverberation of the ultrasound wave can lead to a 1.8-fold increase in the spatial peak, time peak pressure in the head of the rat compared with that in free-field. Because the size of the mouse head is typically smaller than that of rat, this reverberation effect would be more severe in mouse model which needs to be taken into account for choosing an appropriate US exposure condition and also for considering the safety of the animal. Recently, results from Guo et al⁵⁷ and Sato et al⁵⁸ showed US-induced activity patterns to be highly analogous to responses from acoustic stimulus. Their findings also include no apparent US-induced electrophysiological spike activity after removing cochlear aqueduct or transection of the auditory nerves, which raised a challenge on to the direct ultrasonic neuromodulation. Nevertheless, these results do not abolish the neuronal activity responses triggered by US in various types of in vitro preparations, that is, brain slices and peripheral nerves (reviewed in Tyler et al⁵⁹), which do not have cochlear systems. Importantly, the potentially confounding acoustic responses and cross-modal processing in multisensory interaction need to be taken into consideration for those who wish to study direct neuromodulatory responses using ultrasound. Thus, the further research is warranted to understand the fundamental mechanism of ultrasonic neuromodulation.

Conclusion

The experimental observations presented in this study have clearly demonstrated improvement in impaired sensorimotor function compared with those without the LIFU treatment. This can support our hypothesis that enhanced motor execution after the photothrombosis stroke could be attributable to long-term potentiation of hypoactive neural connection between the motor cortex and deep cerebellar nucleus. In our approach, LCN was exposed to US to activate DTC pathway from the beginning of its course which in turn can potentially alleviate the motor impairment. Further studies are necessary to understand synaptic plasticity mechanisms and determine optimal LIFU exposure parameters depending on the severity of the stroke. Our ISI value of 2 seconds was obtained from a previous study where they successfully elicited motor movement in rats.¹⁶ However, considering the overall vulnerability of stroke mouse brain, future studies could benefit from repeated treatment with ISI flexibility for subject variability.

Acknowledgments

We thank Dr Hoon Ryu and Seung Jae Hyeon for conducting hematoxylin and eosin staining and providing the interpretation for the imaging results.

Declaration of Conflicting Interests

The authors declared no potential conflicts of interest with respect to the research, authorship, and/or publication of this article.

Funding

The authors disclosed receipt of the following financial support for the research, authorship, and/or publication of this article: This work was supported by the Korea Institute of Science and Technology Institute Program (2E27980) and the Korea Health Technology R&D Project through the Korea Health Industry Development Institute (KHIDI) funded by the Ministry of Health & Welfare, Republic of Korea (Grant No. HI14C3477).

ORCID iD

Hyungmin Kim  <https://orcid.org/0000-0001-9527-0609>

References

1. World Health Organization. The top 10 causes of death. <http://www.who.int/mediacentre/factsheets/fs310/en/>. Published May 24, 2018. Accessed July 4, 2018.
2. Mozaffarian D, Benjamin EJ, Go AS, et al; American Heart Association Statistics Committee; Stroke Statistics Subcommittee. Heart disease and stroke statistics—2016 update: a report from the American Heart Association. *Circulation*. 2016;133:e38-e360.
3. Hacke W, Kaste M, Bluhmki E, et al; ECASS Investigators. Thrombolysis with alteplase 3 to 4.5 hours after acute ischemic stroke. *N Engl J Med*. 2008;359:1317-1329.
4. Matsuo R, Kamouchi M, Fukuda H, et al. Intravenous thrombolysis with recombinant tissue plasminogen activator for ischemic stroke patients over 80 years old: the Fukuoka Stroke Registry. *PLoS One*. 2014;9:e110444.
5. Wahlgren N, Moreira T, Michel P, et al; ESO-KSU, ESO, ESMINT, ESNR and EAN. Mechanical thrombectomy in acute ischemic stroke: consensus statement by ESO-Karolinska Stroke update 2014/2015, supported by ESO, ESMINT, ESNR and EAN. *Int J Stroke*. 2015;11:134-147.
6. Neumann-Haefelin T, Hoelig S, Berkefeld J, et al; MR Stroke Group. Leukoaraiosis is a risk factor for symptomatic intracerebral hemorrhage after thrombolysis for acute stroke. *Stroke*. 2006;37:2463-2466.
7. Whiteley WN, Slot KB, Fernandes P, Sandercock P, Wardlaw J. Risk factors for intracranial hemorrhage in acute ischemic stroke patients treated with recombinant tissue plasminogen activator: a systematic review and meta-analysis of 55 studies. *Stroke*. 2012;43:2904-2909.
8. Durukan A, Tatlisumak T. Acute ischemic stroke: overview of major experimental rodent models, pathophysiology, and therapy of focal cerebral ischemia. *Pharmacol Biochem Behav*. 2007;87:179-197.

9. Fregni F, Freedman S, Pascual-Leone A. Recent advances in the treatment of chronic pain with non-invasive brain stimulation techniques. *Lancet Neurol.* 2007;6:188-191.
10. Yoo SS, Bystritsky A, Lee JH, et al. Focused ultrasound modulates region-specific brain activity. *Neuroimage.* 2011;56:1267-1275.
11. Tyler WJ, Tufail Y, Finsterwald M, Tauchmann ML, Olson EJ, Majestic C. Remote excitation of neuronal circuits using low-intensity, low-frequency ultrasound. *PLoS One.* 2008;3:e3511.
12. Tufail Y, Matyushov A, Baldwin N, et al. Transcranial pulsed ultrasound stimulates intact brain circuits. *Neuron.* 2010;66:681-694.
13. King RL, Brown JR, Newsome WT, Pauly KB. Effective parameters for ultrasound-induced in vivo neurostimulation. *Ultrasound Med Biol.* 2013;39:312-331.
14. King RL, Brown JR, Pauly KB. Localization of ultrasound-induced in vivo neurostimulation in the mouse model. *Ultrasound Med Biol.* 2014;40:1512-1522.
15. Mehic E, Xu JM, Caler CJ, Coulson NK, Moritz CT, Mourad PD. Increased anatomical specificity of neuromodulation via modulated focused ultrasound. *PLoS One.* 2014;9:e86939.
16. Kim H, Chiu A, Lee SD, Fischer K, Yoo SS. Focused Ultrasound-mediated Non-invasive Brain Stimulation: Examination of Sonication Parameters. *Brain Stimul.* 2014;7:748-56.
17. Younan Y, Deffieux T, Larrat B, Fink M, Tanter M, Aubry JF. Influence of the pressure field distribution in transcranial ultrasonic neurostimulation. *Med Phys.* 2013;40:082902.
18. Guo T, Li H, Lv Y, et al. Pulsed transcranial ultrasound stimulation immediately after the ischemic brain injury is neuroprotective. *IEEE Trans Biomed Eng.* 2015;62:2352-2357.
19. Li H, Sun J, Zhang D, Omire-Mayor D, Lewin PA, Tong S. Low-intensity (400 mW/cm², 500 kHz) pulsed transcranial ultrasound preconditioning may mitigate focal cerebral ischemia in rats. *Brain Stimul.* 2017;10:695-702.
20. Plow EB, Sankarasubramanian V, Cunningham DA, et al. Models to tailor brain stimulation therapies in stroke. *Neural Plast.* 2016;2016:4071620.
21. Plow EB, Machado A. Invasive neurostimulation in stroke rehabilitation. *Neurotherapeutics.* 2014;11:572-582.
22. Levy RM, Harvey RL, Kissela BM, et al. Epidural electrical stimulation for stroke rehabilitation: results of the prospective, multicenter, randomized, single-blinded Everest trial. *Neurorehabil Neural Repair.* 2015;30:107-119.
23. Machado AG, Baker KB, Schuster D, Butler RS, Rezai A. Chronic electrical stimulation of the contralesional lateral cerebellar nucleus enhances recovery of motor function after cerebral ischemia in rats. *Brain Res.* 2009;1280:107-116.
24. Cooperrider J, Furmaga H, Plow E, et al. Chronic deep cerebellar stimulation promotes long-term potentiation, microstructural plasticity, and reorganization of perilesional cortical representation in a rodent model. *J Neurosci.* 2014;34:9040-9050.
25. Shah AM, Ishizaka S, Cheng MY, et al. Optogenetic neuronal stimulation of the lateral cerebellar nucleus promotes persistent functional recovery after stroke. *Sci Rep.* 2017;7:46612.
26. Machado A, Baker KB. Upside down crossed cerebellar diaschisis: proposing chronic stimulation of the dentatohalamo-cortical pathway for post-stroke motor recovery. *Front Integr Neurosci.* 2012;6:20.
27. Gold L, Lauritzen M. Neuronal deactivation explains decreased cerebellar blood flow in response to focal cerebral ischemia or suppressed neocortical function. *Proc Natl Acad Sci U S A.* 2002;99:7699-7704.
28. Elsner B, Kugler J, Pohl M, Mehrholz J. Transcranial direct current stimulation (tDCS) for improving activities of daily living, and physical and cognitive functioning, in people after stroke. *Cochrane Database Syst Rev.* 2016;3:CD009645.
29. Au-Yeung SS, Wang J, Chen Y, Chua E. Transcranial direct current stimulation to primary motor area improves hand dexterity and selective attention in chronic stroke. *Am J Phys Med Rehabil.* 2014;93:1057-1064.
30. Kang N, Summers JJ, Cauraugh JH. Transcranial direct current stimulation facilitates motor learning post-stroke: a systematic review and meta-analysis. *J Neurol Neurosurg Psychiatry.* 2016;87:345-355.
31. Bederson JB, Pitts LH, Tsuji M, Nishimura MC, Davis RL, Bartkowski H. Rat middle cerebral-artery occlusion—evaluation of the model and development of a neurologic examination. *Stroke.* 1986;17:472-476.
32. Franklin KBJ, Paxinos G. *The Mouse Brain in Stereotaxic Coordinates.* 2nd ed. San Diego, CA: Academic Press; 1997.
33. Metz GA, Whishaw IQ. Cortical and subcortical lesions impair skilled walking in the ladder rung walking test: a new task to evaluate fore- and hindlimb stepping, placing, and coordination. *J Neurosci Methods.* 2002;115:169-179.
34. Schallert T. Behavioral tests for preclinical intervention assessment. *NeuroRx.* 2006;3:497-504.
35. Bouet V, Boulouard M, Toutain J, et al. The adhesive removal test: a sensitive method to assess sensorimotor deficits in mice. *Nat Protoc.* 2009;4:1560-1564.
36. Keep RF, Hua Y, Xi G. Brain water content. A misunderstood measurement? *Transl Stroke Res.* 2012;3:263-265.
37. Kleim JA, Barbay S, Nudo RJ. Functional reorganization of the rat motor cortex following motor skill learning. *J Neurophysiol.* 1998;80:3321-3325.
38. Nudo RJ, Milliken GW. Reorganization of movement representations in primary motor cortex following focal ischemic infarcts in adult squirrel monkeys. *J Neurophysiol.* 1996;75:2144-2149.
39. Frost SB, Barbay S, Friel KM, Plautz EJ, Nudo RJ. Reorganization of remote cortical regions after ischemic brain injury: a potential substrate for stroke recovery. *J Neurophysiol.* 2003;89:3205-3214.
40. Liepert J, Bauder H, Wolfgang HR, Miltner WH, Taub E, Weiller C. Treatment-induced cortical reorganization after stroke in humans. *Stroke.* 2000;31:1210-1216.
41. Liepert J, Uhde I, Gräf S, Leidner O, Weiller C. Motor cortex plasticity during forced-use therapy in stroke patients: a preliminary study. *J Neurol.* 2001;248:315-321.
42. Tarkka IM, Kononen M, Pitkanen K, Sivenius J, Mervaala E. Alterations in cortical excitability in chronic stroke after constraint-induced movement therapy. *Neurol Res.* 2008;30:504-510.
43. Baker KB, Schuster D, Cooperrider J, Machado AG. Deep brain stimulation of the lateral cerebellar nucleus produces frequency-specific alterations in motor evoked potentials in the rat in vivo. *Exp Neurol.* 2010;226:259-264.

44. Hayashibe M, Zhang Q, Guiraud D, Fattal C. Evoked EMG-based torque prediction under muscle fatigue in implanted neural stimulation. *J Neural Eng.* 2011;8:064001.
45. Kapur N. Paradoxical functional facilitation in brain-behaviour research. A critical review. *Brain.* 1996;119(pt 5):1775-1790.
46. Furlan M, Marchal G, Viader F, Derlon JM, Baron JC. Spontaneous neurological recovery after stroke and the fate of the ischemic penumbra. *Ann Neurol.* 1996;40:216-226.
47. Bonow RH, Silber JR, Enzmann DR, Beauchamp NJ, Ellenbogen RG, Mourad PD. Towards use of MRI-guided ultrasound for treating cerebral vasospasm. *J Ther Ultrasound.* 2016;4:6.
48. Popa T, Velayudhan B, Hubsch C, et al. Cerebellar processing of sensory inputs primes motor cortex plasticity. *Cereb Cortex.* 2013;23:305-314.
49. Proville RD, Spolidoro M, Guyon N, et al. Cerebellum involvement in cortical sensorimotor circuits for the control of voluntary movements. *Nat Neurosci.* 2014;17:1233-1239.
50. Schulz R, Frey BM, Koch P, et al. Cortico-cerebellar structural connectivity is related to residual motor output in chronic stroke. *Cereb Cortex.* 2017;27:635-645.
51. Kim H, Lee SD, Chiu A, Yoo SS, Park S. Estimation of the spatial profile of neuromodulation and the temporal latency in motor responses induced by focused ultrasound brain stimulation. *Neuroreport.* 2014;25:475-479.
52. Kamimura HAS, Wang S, Chen H, et al. Focused ultrasound neuromodulation of cortical and subcortical brain structures using 1.9 MHz. *Med Phys.* 2016;43:5730-5735.
53. Gaffield MA, Christie JM. Movement rate is encoded and influenced by widespread, coherent activity of cerebellar molecular layer interneurons. *J Neurosci.* 2017;37:4751-4765.
54. Duck FA. Medical and non-medical protection standards for ultrasound and infrasound. *Prog Biophys Mol Biol.* 2007;93:176-191.
55. Wahab RA, Choi M, Liu YB, Krauthamer V, Zderic V, Myers MR. Mechanical bioeffects of pulsed high intensity focused ultrasound on a simple neural model. *Med Phys.* 2012;39:4274-4283.
56. Dewhirst MW, Viglianti BL, Lora-Michiels M, Hanson M, Hoopes PJ. Basic principles of thermal dosimetry and thermal thresholds for tissue damage from hyperthermia. *Int J Hyperthermia.* 2003;19:267-294.
57. Guo H, Hamilton M 2nd, Offutt SJ, et al. Ultrasound produces extensive brain activation via a cochlear pathway. *Neuron.* 2018;98:1020-1030.e4.
58. Sato T, Shapiro MG, Tsao DY. Ultrasonic neuromodulation causes widespread cortical activation via an indirect auditory mechanism. *Neuron.* 2018;98:1031-1041.e5.
59. Tyler WJ, Lani SW, Hwang GM. Ultrasonic modulation of neural circuit activity. *Curr Opin Neurobiol.* 2018;50:222-231.